Nigerian Journal of Technology
Vol. 40, No. 3, May, 2021, pp. 501–517.
www.nijotech.com

Print ISSN: 0331-8443
Electronic ISSN: 2467-8821
http://dx.doi.org/10.4314/njt.v40i3.16

Analysis of the Electronic Circuits of 11 W and 15 W Compact Fluorescent Lamps

M. A. Adelabu[a], A. L. Imoize[a,b,*], G. U. Ughegbe[a]

[a]*Department of Electrical and Electronics Engineering, Faculty of Engineering, University of Lagos, 100213 Akoka, Lagos, NIGERIA.*
[b]*Department of Electrical Engineering and Information Technology, Institute of Digital Communication, Ruhr University, 44801 Bochum, GERMANY.*

Abstract

The introduction of electronic ballast in lighting systems design has dramatically revolutionized the lighting space. This is orchestrated by the entrance of the Compact Fluorescent Lamps (CFLs) and Light Emitting Diodes (LEDs) into the lighting market. The CFLs currently being used in domestic and industrial lighting systems provide highly competitive alternatives to conventional incandescent lamps. The electronic ballast incorporated into the CFLs helps eliminate the flickering and slow starting flaws prevalent in traditional fluorescent lamps. To properly evaluate the performance characteristics and limitations of the CFLs, a critical analysis of its electronic circuit becomes imperative. To this end, this paper presents experimental and simulation analyses of the CFL circuits. To achieve this, two Futina CFL bulbs of 11W and 15W model YPZ220/11-BMSP RR/RDD and YPZ220/15-BMSP RR/RDD, respectively, were analyzed and experimentally verified. A function-based programming paradigm was applied to develop a graphical user interface (GUI) used for the circuits analyses. The GUI is designed using MATLAB graphical user interface development environment (GUIDE). Experiments were conducted to obtain the performance characteristics of the CFLs, and measurements show that the 11W lamp has a higher amplitude than the 15W lamp. However, both lamps show similar waveforms after 300 seconds. The maximum voltage amplitudes for both CFLs are the same, with a peak value of 218V. The current waveforms in the spectral domain gave a maximum amplitude of 0.3 A for the 11W CFL and 0.2 A for the 15W. The voltage frequency (0.00196) of both CFLs are the same, whereas the current frequencies are different. This indicates that the wattage of a CFL does not affect the frequency of its voltage waveform. The frequency of the 11W CFL current (0.00157) is higher than that of the 15W CFL current (0.00784). This implies that the higher the CFL wattage, the lower the frequency of its current waveform. Additionally, simulation results revealed that the key difference between the CFLs is the current total harmonic distortion (THDI), which increases with an increasing rated power of the CFL or the aggregation of a number of the smaller rated CFLs.

Keywords: 11W and 15W CFLs, AC and DC analysis, compact fluorescent lamps, current and voltage waveforms, electronic ballast, Total harmonic distortion

1. INTRODUCTION

The increasing popularity of the Compact Fluorescent Lamps (CFLs) over the conventional incandescent lamps in the various household, security, and industrial outlets fuel the need to investigate its electronic circuit. There are two main parts in a CFL: the gas-filled tube (burner) and the electronic ballast. This study aims to describe and analyze how the CFL electronic circuit (electronic ballast) works with its associated components. However, the gas-filled tube (mercury gas inside the spiral component) is not the focus of this investigation. In the existing literature, several efforts have been made to provide the working principles of the electronic ballast and possibly develop a cost-effective alternative [1–3]. This led to the development of the local silicon-controlled-rectifier inverters for lamps and the high-frequency rotating AC generators for the large banks of lamps commonly found in homes and industrial buildings. As the primary components used for the CFL design, such as the transistor and ferrite, AC and DC inverters become ubiquitous. Thus, it becomes very easy to obtain DC and AC inverters suitable for the design, analysis, and applications of the electronic ballast.

Additionally, adequate lighting is essential for residential and industrial buildings. Most households and industrial environments have moved

*Corresponding author (**Tel:** +234(0) 706 783 4077)
Email addresses: madelabu@unilag.edu.ng (M. A. Adelabu), aimoize@unilag.edu.ng (A. L. Imoize), gloryughegbe@yahoo.com (G. U. Ughegbe)

away from using incandescent lamps (ILs) as the means of illuminating their environments to using fluorescent (FL) tubes and CFL lamps. The motivation is the power consumed by both the FLs and CFLs is significantly lower than that consumed by the ILs for the same amount of luminance. However, it has been observed that the use of FLs and CFLs introduces harmonics into the system which can affect other electronic and electrical devices connected to the same source/supply. In this study, the total harmonic distortion (THD) as a result of connecting a CFL is examined. FUTINA 11 W and FUTINA 15 W CFL circuits were implemented via simulation and experimentation to investigate their associated THDs and other characteristics. Thus, the electronic ballasts of the CFLs are implemented.

Additionally, the use of the electronic ballast in the CFLs design lends credence to their energy-saving capabilities and the ease of eliminating possible light flickering effects. Electronic ballasts also aid versatile lamp control and help mitigate the impact of start-up vibrations in the CFLs [4]. Also, the replacement of magnetic ballasts with electronic ballasts has led to enormous savings in energy [5, 6]. For example, an average of 14 Watts is saved for the fluorescent tubes of 36 Watts, and 7 Watts savings have been observed for the fluorescent tubes of 18 Watts [7, 8]. Further to this, the reliability of the electronic ballast could be traceable to their ages [9]. The more time it spends in active service, the lower its chances of failing. Hence, the first six months may be regarded as the incubation period for the electronic ballast.

In the works of literature, a few analyses of the electronic ballast have been presented [10, 11]. Most of such analyses were streamlined and lacked adequate information to understand its working principles fully. Toward this end, the need to present a rigorous analysis of the electronic circuit of the ballast becomes imperative. Thus, this paper aims to present a robust analysis of the electronic ballast circuits, emphasizing the DC and AC characteristics. The main contributions of this paper are as follows;

1. An extensive experimental and simulation analyses of the electronic circuits of two CFLs model YPZ220/11-BMSP RR/RDD and YPZ220/15-BMSP RR/RDD.

2. Comparison of the selected CFLs model (YPZ220/11-BMSP RR/RDD and YPZ220/15-BMSP RR/RDD) to evaluate their electrical characteristics.

3. Application of a function-based programming paradigm to write codes in MATLAB to develop a graphical user interface (GUI). This is designed using MATLAB graphical user interface development environment (GUIDE).

4. The analyses of the current and voltage waveforms of the CFLs were carried out in the spectral domain and the simulated results were compared with the experimental measurement.

The remainder of this paper is organized as follows. Section 2 reports the related work. Section 3 presents the materials and methods. Section 4 presents the results and discussions. Finally, the conclusion to the paper is given in Section 5.

2. RELATED WORK

In the existing works of literature, several researchers have presented investigations on the characteristics of CFLs. Some of these works examined the potential benefits and prospects of the CFLs while others assessed the various degrees of hazards posed by the CFLs [12–19]. Specifically, the work in [12] compares the CFL and incandescent lamps in the field of life cycle assessment (LCA). Similarly, a comparative analysis between the compact fluorescent lamps and conventional filament lamps is presented in [13]. In [14], a novel self-oscillating Class E ballast from a design point of view was proposed. Furthermore, laboratory tests were performed on more than 23 brands of CFLs to understand their electrical performances in [15]. Additionally, a frequency-domain harmonic model for the CFL was proposed in [16]. Furthermore, the feasibility of causing physical harm through the explosion of CFLs to home occupants was conducted through the exploitation of the home automation system [17]. In [18], spent compact fluorescent lamps were characterized to determine the distribution of mercury. Additionally, exposure analysis of the accidental release of mercury from compact fluorescent lamps was investigated in [19].

It is worthy of note that the harmonic distortion characteristics of CFLs on electrical distribution systems are evaluated and analyzed by Khan et al. [20]. The CFL penetration levels in terms of their harmonic distortions under varying conditions were determined. The Electro-Magnetic Transients Program (EMTP) was used to evaluate the harmonic cancellation effects. The characteristics of the frequency response and the distribution system were examined as well. The EMTP simulations created models using the frequency versus the applied loads on the system frequency response characteristics. Results obtained showed a correlation of CFL current distortion levels with their penetrating abilities. According to Dalla Costa et al. [21], losses on an electronic ballast are tested to ascertain its performance, using eight different ballast topologies. The losses at the various points across the ballast with or without a PFC filter or oscillating driver were evaluated. Waveforms from the ballast were used to assess the losses, performance, and preventive actions to reduce the losses.

Furthermore, the electronic ballast circuit of a dimmable compact fluorescent lamp is designed and developed by Tam et al. [22]. The work aims to address the compatibility issues attributed to triac dimmers and achieve an acceptable low-cost electronic ballast. To arrive at the final dimmable

circuit, different topologies and operational modes were evaluated. A 16W dimmable prototype was simulated using Spice to derive the required components parameters and values. With this, a low-cost design was achieved, and it passed the compatibility test with traditional dimmers. However, the dimming operations of this model are not dependent on the voltage control mechanism. In Parsons et al. [23], the environmental impact in terms of the strengths and limitations of CFLs and Incandescent Lamps in the Australian environment is investigated. The chemical/gases (mercury, lead, phosphor, and argon) components of the lamps were hazardous to the Australian environment. Further, a comparison of the environmental impact of both lamps was represented on bar and pie charts, respectively. The harmonic distortion effects, low power factor, and electromagnetic interference associated with these lamps were highlighted.

Additionally, the behavioral pattern of CFLs current and voltage waveforms using 12 CFLs samples is investigated by Cunill-Solà and Salichs [24]. The goal is to study the distortion level and impact of each current waveform on the quality of the voltage waveform. The PSpice simulation program was employed to model and simulate the behavior of the electrical waveforms. A comparison of actual measurements and simulated values was carried out to validate the negative impact of current waveform distortion on the voltage waveform. The lamps harmonic decomposition and distortion percentages were observed. However, the study did not consider CFLs above 25W.

In another related study, a single-stage high-power-factor electronic ballast designed for a Compact Fluorescent Lamp is reported by Lam and Jain [25]. This was achieved using an electronic ballast that operates at a higher frequency of above 25kHz and includes a power-factor-correction component on a 13W CFL. The harmonics, current, and voltage analysis, among others, for the proposed circuit was reported. The current and voltage waveforms were plotted and analyzed, and the proposed circuit was simulated using PSIM 7.0 software. Also, the behavior of the lamp at the preheat and ignition stages was analyzed. Theoretical analysis is replicated with mathematical derivations using the applied circuit parameters. Results showed that the desired power factor and efficiency were achieved. However, some of the circuit components were assumed to be lossless, which may not hold in most practical scenarios.

In Matvoz and Maksić [26], the negative impact of CFLs harmonic currents and voltages on the electric power network is investigated. Eight (8) samples of CFLs were used for the study to measure the parameters of different power functions and harmonic currents. These parameters were used to develop a model, which was simulated using the PSCAD program, considering two scenarios (incandescent light bulb and CFLs) for comparison. The purpose of the harmonic analysis of the voltages is to determine the potential impact of the CFLs on the tested power network. The work showed that dealing with the harmonics in electric power networks is cost-prohibitive. An extensive assessment of the environmental impact of CFL and Incandescent lamps is presented by Ramroth [27]. The work used the Life-Cycle Analysis (LCA). This involves "cradle-to-grave" analysis of both lamps, comparing their physical, chemical components, and intrinsic features. Additionally, Matvoz and Maksić [28] compared the impact of light-emitting diodes (LED) lamps on a simulated distribution system with that of the CFLs on the system. Several samples of the LED lamps were tested on the electricity network. PSCAD software was used to simulate the LED measurements under different load conditions. These include active power from the high voltage (HV) network, reactive power, power factor, and total harmonic distortion (THD). Results showed a similarity of reducing network losses among others. However, not all the lamps were consistent with the harmonic measurements. Additionally, the high cost of providing a medium or low voltage (MV/LV) transformer for harmonics control could pose a significant setback to the practical application of the proposed scheme.

Similarly, electronic ballast with a passive valley-fill power factor correction component is proposed for CFL Lightings by Lam, Pan, and Jain [4]. A passive power-factor correction component was included in the electronic ballast. The electronic ballast shows a high cost of production and very large. The characteristics and analysis of each stage of the ballast were analyzed. Circuit variables and parameters were processed in MATLAB, and the proposed circuit is simulated using PSIM 9.1 software. A built prototype enabled the simulation test and results. Each stage of the proposed electronic ballast was mathematically presented. Results obtained from the experiments and simulations affirmed the importance of the proposed circuit. However, the PFC component tends to induce a high lamp current.

The technical requirements for achieving a low-cost electronic ballast using simple control circuits and implementing simple circuit topologies are reported by Ribarich and Ribarich [29]. Although the various parts of the electronic ballast are highlighted, the focus is on the control circuit. Two electronic ballasts with PFC of 54W and without PFC of 26W were designed and compared. Results indicate that both PFC and non-PFC electronic ballast performed optimally. However, PFC circuits tend to add to the cost, energy consumption, and electronic ballast size. The harmonic disturbance in electronic ballast is modeled using the EMTP/ATP program for CFLs by Oramus, Smugała, and Zydroń [30]. The work investigates the impact of high harmonics from CFLs on distribution systems. Eleven samples of CFLs harmonics pattern and behavior on current waveforms were analyzed, and a model of the CFL is generated from the EMTP/ATP program for comparison. The measured and calculated waveforms showed similarity in behavior. However, the de-

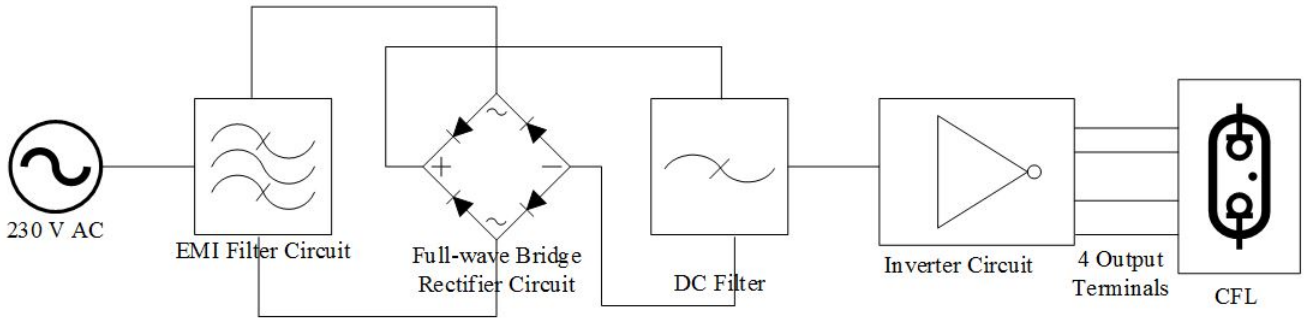

Figure 1: General circuit diagram pattern for the CFL electronic ballast.

veloped model shows limited applications in high-voltage distribution systems.

The need for PFC in CFLs and LEDs to compensate for lagging power factor of below 0.64 and total harmonic distortion of over 136% in lighting applications is presented by Revelo-Fuelagán [31]. This is achieved by adding a PFC controller to the CFL electronic ballast and the circuit of the LED with a hysteretic control. The PFC analysis for the CFL and LED is done using numerical simulations and experimental results for validation. Other parameters considered for the CFL are the switching times with and without PFC. For the LED lamp, the simulation results were obtained using PSIM software, and the prototype provided the experimental result. Providing the economic benefits of low-cost, low power consumption, and small PFC controller was achieved for both lights. However, achieving an accurate signal flow was practically difficult in the prototype.

The preceding literature revealed that the analysis of the current and voltage waveforms in the spectral domain for the CFLs had not been given adequate coverage. Thus, this study aims to fill this gap. The goal is to analyze the current and voltage waveforms in the spectral domain via computer simulation and compare the results with experimental measurements. The materials and methodology are described in Section 3 of this paper.

3. MATERIALS AND METHODS

The materials and methods used in the circuit analysis are presented in this Section. The materials used are presented in Section 3.1, and the methodology is described comprehensively in Section 3.2.

3.1. Materials

The materials used for this study comprise the CFL electronic ballast, the EMI filter, the rectifier circuit, the power factor correction circuit, the half-bridge resonant circuit, and the control unit. These are briefly described as follows.

3.1.1. The CFL electronic ballast

The essential components of an electronic ballast are the EMI filter, rectifier, PFC, half-bridge resonant output, and control unit, as illustrated in Fig. 1. Other useful components are embedded in the five essential parts. It is estimated that an average CFL will yield a brightness of 63.735 lumens per watt while an average IL will yield a brightness of 14.5 lumens per watt. This implies that the 11 W CFL will replace 50 W IL and 15 W CFL will replace 65 W IL. In general, a CFL e-ballast follows the same circuit arrangement as shown in Fig. 1. A small resistor (FUTINA 11 W), up to 22 Ω, or a fuse (FUTINA 15 W) is usually connected in series between the AC source and the electromagnetic interference (EMI) filter circuit to limit overload and short-circuit current. The EMI filter circuit reduces the electromagnetic interference from the input. It is mostly implemented with an inductor in series and a capacitor in parallel. The full-wave bridge rectifier circuit is used to convert AC to DC. It consists of four P-N junction diodes. The DC filter is usually done filter a polarized capacitor connected in parallel with the output of the full-wave rectifier for filtering purposes. Thereafter, an inverter circuit using two NPN bipolar transistors is used as the inverter circuit. The transistors create a high-frequency square wave AC signal. A choke is usually connected to the output of the inverter to increase the voltage at starting time to about 1000 V. Once the CFL bulb is on, the voltage across the CFL decreases to about 230 V, and the current flows into the CFL decreases accordingly. The voltage source can be modeled using Eq. 1. Further explanations on the circuit components are given in Sections 3.1.2 – 3.1.6.

$$V = V_0 \sin(2\pi f t + \phi) \tag{1}$$

where V_0 is the peak voltage amplitude in volts; f is the frequency in Hertz; t is the time in seconds and ϕ is the phase shift in radians. The peak voltage (V_0) can be expressed with Eq. (2).

$$V_0 = V_{rms}\sqrt{2} \tag{2}$$

The DC voltage after rectification is the peak voltage less voltage drop. A full-wave bridge rectifier that uses four NPN junction diodes were used. During the positive cycle of the AC voltage, the voltage passes through two diodes. Similarly, during the negative cycle of the AC voltage, the voltage passes through the other two diodes. Therefore, the voltage drop can be expressed with Eq. 3.

$$V_{drop} = 2V_f \tag{3}$$

V_f is the forward voltage of each diode. This implies that the DC voltage can be expressed with Eq. 4.

$$V_{dc} = V_0 - V_{drop} \tag{4}$$

3.1.2. The EMI filter

The EMI filter blocks off any existing electromagnetic interference (EMI). EMI can either be conducted or the radiated type. When noise travels through electrical conductors and wires, it is called conducted EMI. Radiated EMI entails traveling through a free space or air interface. In other words, the EMI filter circuit suppresses EMI interference induced by conduction and radiation. For the electronic ballast, the problem of electromagnetic compatibility is to prevent the high-frequency signal conducted out through the power line and interferes with the operation of other electrical equipment. The EMI filter circuit is composed of a capacitor, an inductor, and a resistor. It can also be called radio-frequency interference filters. It is a passive two-way circuit consisting of the power supply (line) and the load. EMI filter is an impedance matching circuit. The greater the impedance adaptation between the input and output sides of the EMI filter and the power supply and load side, the more effective the attenuation of electromagnetic interference is. The filter can effectively filter out the frequency of a specific frequency band in the power line or the outside frequency to obtain a particular frequency or eliminate the power signal after a specific frequency point.

3.1.3. The rectifier circuit

The rectifier is the main component responsible for AC power to DC power conversion. It is made up of diodes.

3.1.4. Power factor correction circuit

The Power Factor Correction (PFC) circuit is referred to as the valley-fill circuit. Losses can be inevitable due to the introduction of the Power Factor. Power Factor Correction is achieved by increasing the charge time of capacitors. The connection of many electronic ballasts to AC mains increases the total peak current. It becomes a significant problem because of higher power line losses, higher-capacity power delivery equipment, and wasted electricity and voltage fluctuations. The Power factor correction circuit (PFC) is required to "correct" these loads to have a high-power factor, more resistive, and require lesser peak currents.

3.1.5. Half-bridge resonant output

It converts DC to square waved voltage with high frequency ranging from (20KHz to 80KHz).

3.1.6. Control unit

This controls the voltage and current across and through the CFL.

3.2. Methodology

The methodology used in the electronic ballast circuit analysis is described in this section. The various compositions are described in Sections 3.2.1 – 3.2.7.

3.2.1. Compact fluorescent lamps

The selected CFLs are the YPZ220/11-BMSP RR/RDD and YPZ220/15-BMSP RR/RDD Futina products from China. Their circuits were analyzed by identifying each component with their respective values. The digital multimeter was used to test the condition of the lamps' components and measure the output voltages of the power supply. After that, the 11W and 15W circuits analyses and modeling were carried out in MATLAB, a Mathworks Incorporated product. The 15W CFL was also simulated using Multisim software for the comparison of results. Two FUTINA CFL lamps were selected for the electronic ballast analysis based on availability and cost-efficiency. The electronic ballast of the 11W and 15W CFLs is as shown in Fig. 2(a).

3.2.2. Circuit analysis

The following data was collected for analysis. DC and AC waveforms, harmonics waveforms, voltage, current waveforms, line current at rated voltage waveforms, active power by varying the supply voltage graph, and power factor (PF) vary the supply voltage harmonics current spectrum in percentage with different power ratings.

3.2.3. Electronic circuit testing

The testing and simulation were done with MATLAB and Simulink, and a digital multimeter. The electronic circuit diagrams of the tested 11W and 15W CFLs are given in Fig. 2(b) and Fig. 2(c), respectively.

3.2.4. Experimental measurements

We collected voltage and current waveforms of two different CFL lamps. The first lamp is an 11W Futina lamp, while the second is a 15W Futina lamp. Each lamp is connected to a 220V AC source. The voltage and current reading are measured with a caliper clamp multimeter and recorded at a 5 seconds interval. The total records for each lamp are 102.

3.2.5. MATLAB/Simulink implementation

The electronic circuits of the selected CFLs (YPZ220/11-BMSP RR/RDD and YPZ220/15-BMSP RR/RDD) and their chosen components comprising of resistors, capacitors, inductors, diodes, and transistors with their specified values were modeled and simulated in MATLAB. The

(a) Electronic Ballast of the 11W and 15W CFLs

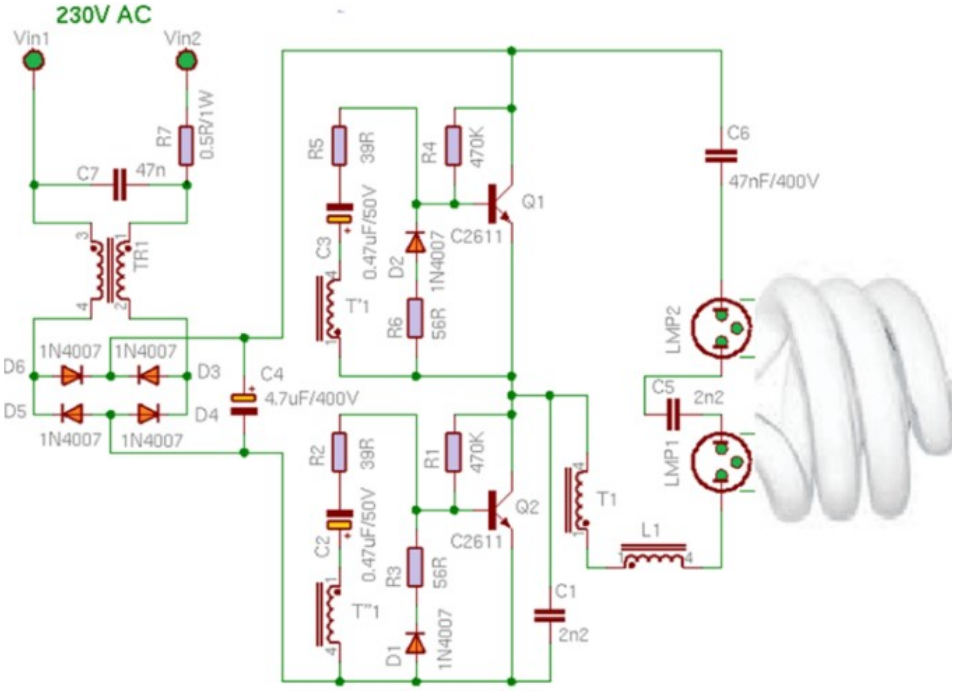

(b) Circuit Diagram of the 11W CFL

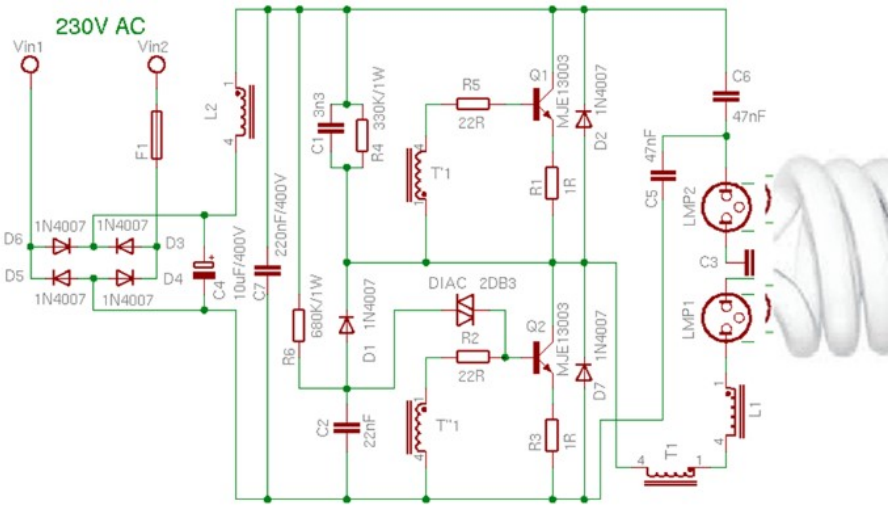

(c) Circuit Diagram of the 15W CFL

Figure 2: (a) Electronic Ballast of the 11W and 15W CFLs; (b) Circuit Diagram of the 11W CFL; (c) Circuit Diagram of the 15W CFL.

Table 1: Basic parameters of the tested CFLs.

S/N	Model	Power (W)	Luminous Flux (lm)	Colour (K)	Base Type
CFL-01	YPZ220/11-BMSP RR/RDD	11	550	6400	B22
CFL-02	YPZ220/15-BMSP RR/RDD	15	750	6400	B22

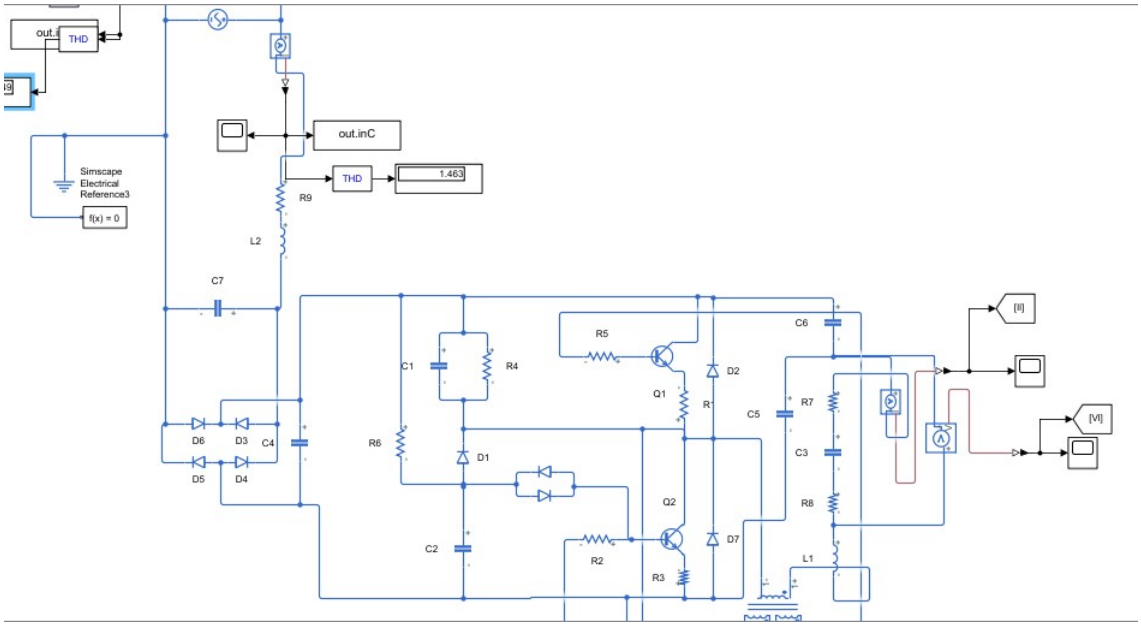

(a) 11W CFL MATLAB/Simulink implementation

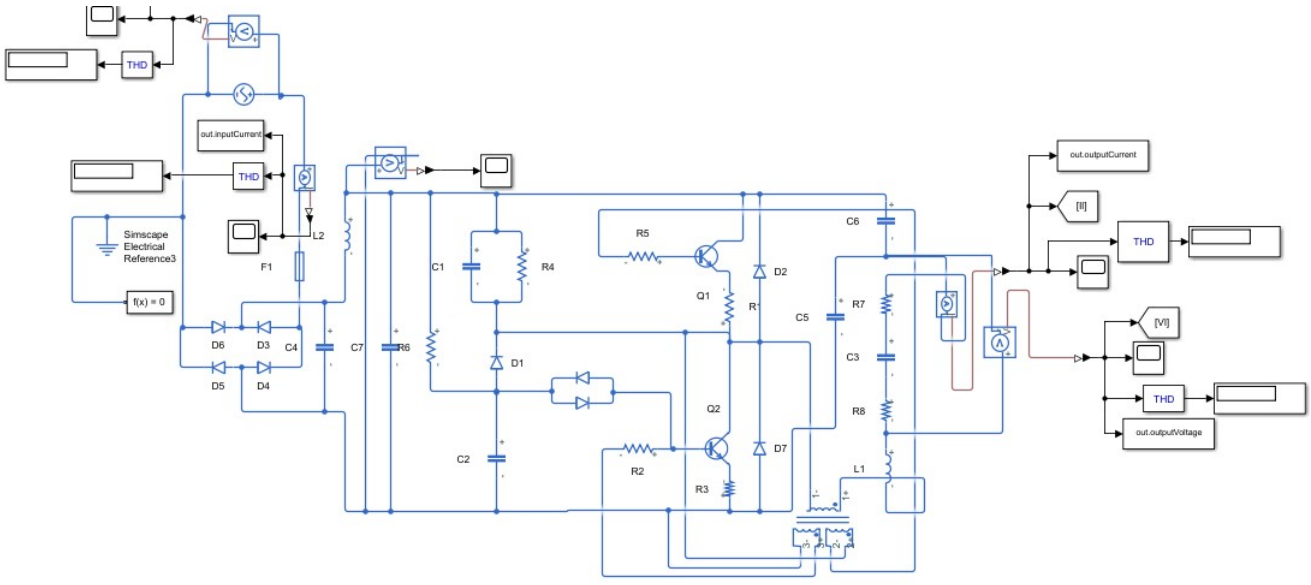

(b) 15 W CFL MATLAB/Simulink implementation

Figure 3: (a) 11W CFL MATLAB/Simulink implementation; (b) 15 W CFL MATLAB/Simulink implementation

basic parameters of the tested CFLs are given in Table 1. The MATLAB/Simulink implementation for the FUTINA 15 W CFL and FUTINA 11 W CFL are shown in Figs. 3(a) and 3(b), respectively.

3.2.6. Software development

In this work, we developed an application in MATLAB. The application has a graphical user interface (GUI) designed using MATLAB graphical user interface development environment (GUIDE). A function-based programming paradigm is used in writing the codes with MATLAB version R2016A. The application GUI allows a user to import signal data in an excel file into the application. There is no limit to the number of unique CFL data that can be imported. Each CFL data should be in a separate excel sheet. The application makes it easy to filter each CFL data or compare them. Well-labeled graphs are generated with the click of buttons. Figure 4 shows the interface of the application.

3.2.7. Signal filtering

To remove the noise in the voltage and current waveforms, a fast Fourier-transform is applied. Fast Fourier-transform converts the signal from a time domain into a frequency/spectral domain. The next step is to compute the spectral-domain signal amplitude and fix all amplitudes less than 95% to zero. After filtering the spectral signal, an inverse Fourier-transform is applied to obtain the filtered time-domain data. Figure 5 shows a flowchart description of the filtering process. The results and discussions of the circuit analyses are given in Section 4 of this paper.

4. RESULTS AND DISCUSSION

In this section, the results of the electronic circuit analysis are presented. First, the experimental results are reported in Section 4.1 and the Simulink model results of the CFL circuits are given in Section 4.2. Last, the results are discussed in Section 4.3 of this paper.

4.1. Results of the Experimental CFL Circuits Analysis

The results of the electronic circuit analysis of the two CFLs are presented in this section. Figure 6(a) gives the 11W and 15W Voltage Waveforms, and Fig. 6(b) shows the 11W and 15W Current Waveforms. Fig. 7(a) represents the Harmonic Voltage Spectrum of the 11W and 15W CFLs, and Fig. 7(b) shows the harmonic current spectrum of the 11W and 15W CFLs. Further, a comparison of the original voltage waveforms with the filtered waveforms is given in Fig. 8(a). Additionally, a comparison of the original current waveforms with the filtered waveforms shown in Fig. 8(b). These results are briefly discussed in section 4.2. The filtered signals in Figs. 8(a) and 8(b) can be expressed in Eq. (5) and (6) for the voltages and currents, respectively.

$$V_{11} = 217.89 - 0.4878\cos(2\pi \times 0.00196 \times t) \quad (5a)$$

$$V_{15} = 217.47 - 0.9535\sin(2\pi \times 0.00196 \times t) \quad (5b)$$

$$I_{11} = 0.2957 + 0.0076\sin(2\pi \times 0.0157 \times t) \quad (6a)$$

$$I_{15} = 0.20137 + 0.011239\cos(2\pi \times 0.00784 \times t) \quad (6b)$$

4.2. Simulink Model Results of the CFL Circuits

In this section, the Simulink model results of the CFL circuits are presented. First, the 11W CFL source response is given in Section 4.2.1 and the 15W CFL source response is presented in Section 4.2.2.

4.2.1. The 11 W CFL source response

The results for the 11W CFL source response are presented in this section. Figure 9(a) gives the source voltage for the 11 W CFL. Figure 9(b) provides the source current for the 11 W CFL, and Figure 9(c) shows the zoomed source current waveform for the 11 W CFL during running.

4.2.2. The 15 W CFL source response

The results for the 15 W CFL source response are presented in this section. Figure 10(a) gives the voltage supply waveform for the 15 W CFL. Figure 10(b) shows the output voltage of the full-wave rectifier for the 15 W CFL. Figure 10(c) provides the source current waveform for the 15 W CFL. Figure 10(d) shows the source waveform for the 15 W CFL during the running stage. Finally, Figure 10(e) gives the zoomed source current waveform of the 15 W CFL during the running stage. Finally, the performance comparison of the tested 11W and 15W CFLs is given in Table 2.

Table 2: Performance comparison of the investigated 11W and 15W CFLs.

Parameter	11 W CFL	15 W CFL
Percentage THDV	2.908%	0.001%
THDV (dB)	0.249	9.069×10^{-5}
Percentage THDI	18.345%	98.404%
THDI (dB)	1.463	5.951
Time to steady-state (ms)	5	5

4.3. Discussion of Results

In the preceding section, the experimental and simulation results of the electronic circuits analyses are presented in Figs. 6 – 10. In particular, Fig. 6(a) shows the voltage waveforms of both 11W and 15W lamps. As seen in Fig. 6(a), both lamps have similar waveforms after 300 seconds. Fig. 6(b) represents the current waveforms of the 11W and 15W lamps. It is clear from Fig. 6(b) that the 11W lamp has a higher amplitude than the 15W lamp. Fig. 7(a) shows the voltage waveforms in the spectral domain. It is clear from Fig. 7(a) that the maximum voltage amplitudes for both 11W and 15W CFLs are the same. The

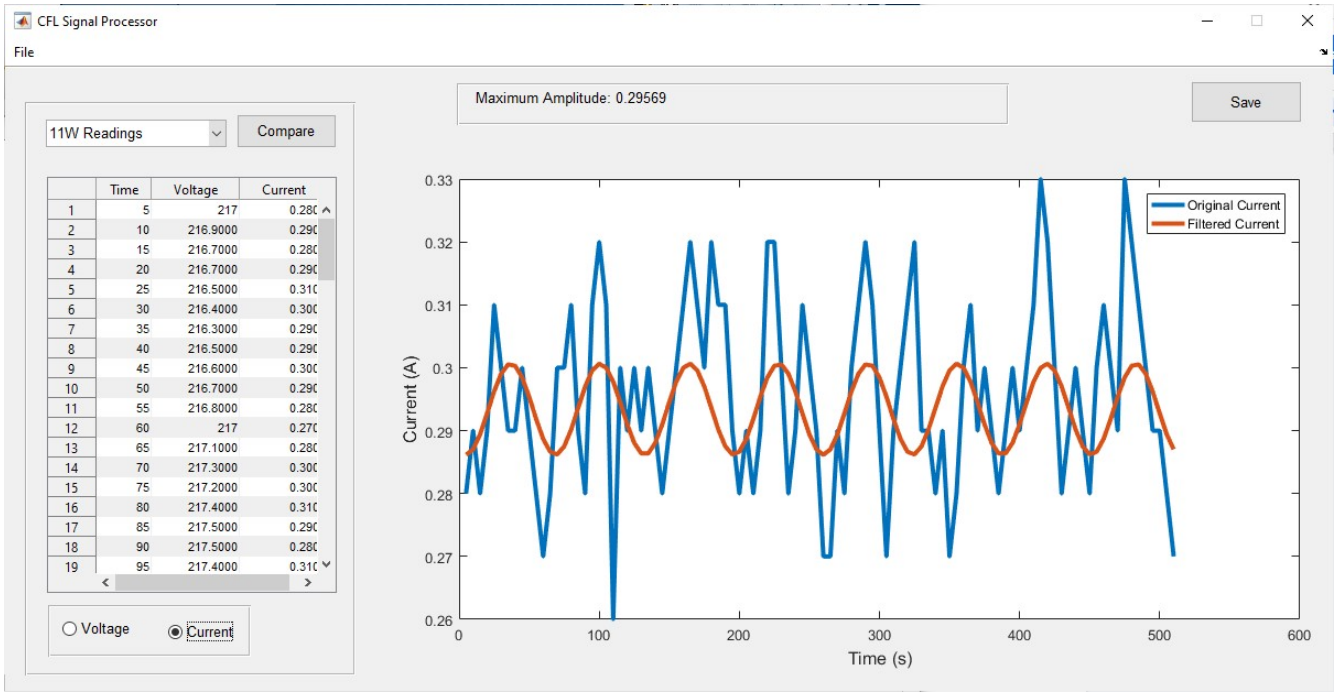

Figure 4: Software interface of the developed GUI for electronic circuits analysis.

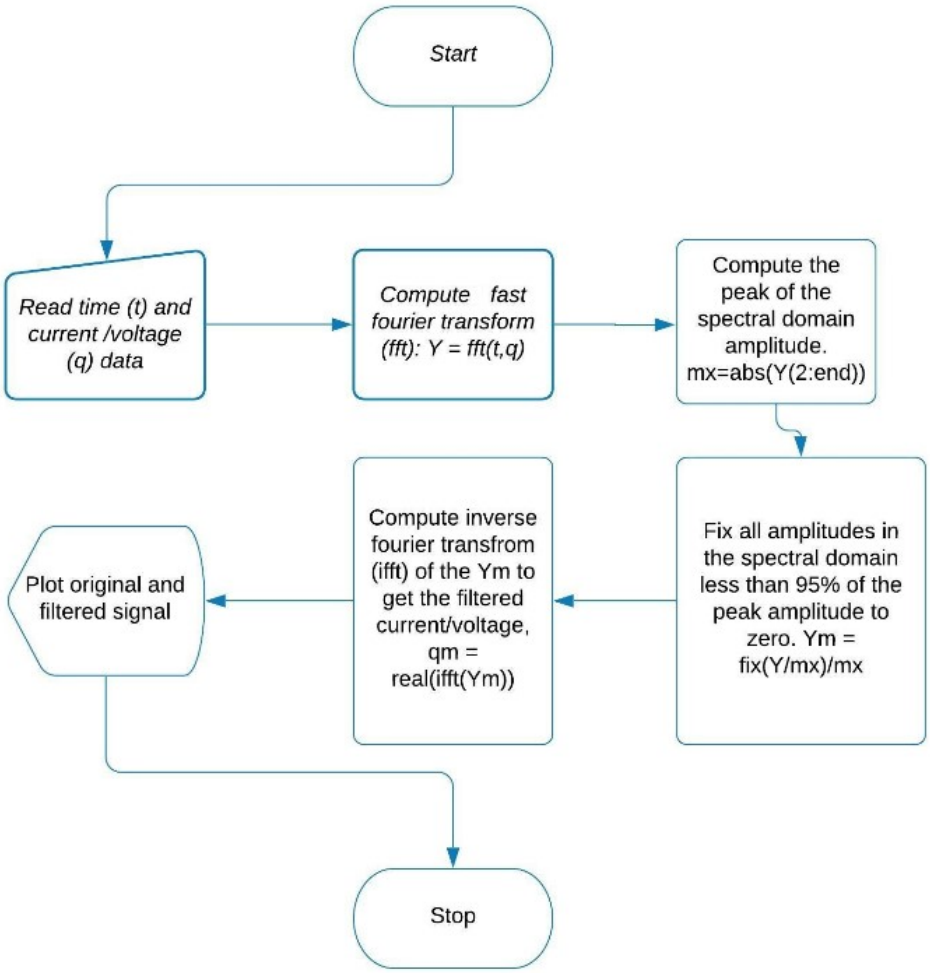

Figure 5: Flowchart describing how the current and voltage waveforms are filtered.

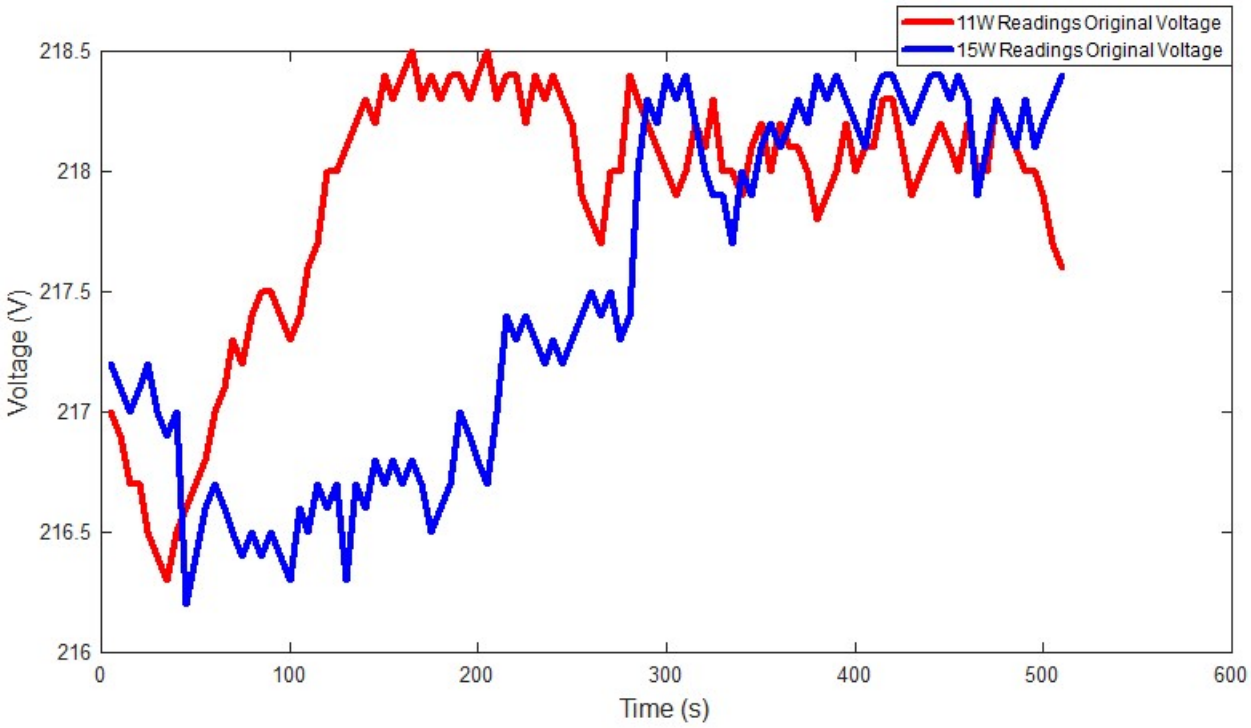

(a) 11W and 15W Voltage Waveforms

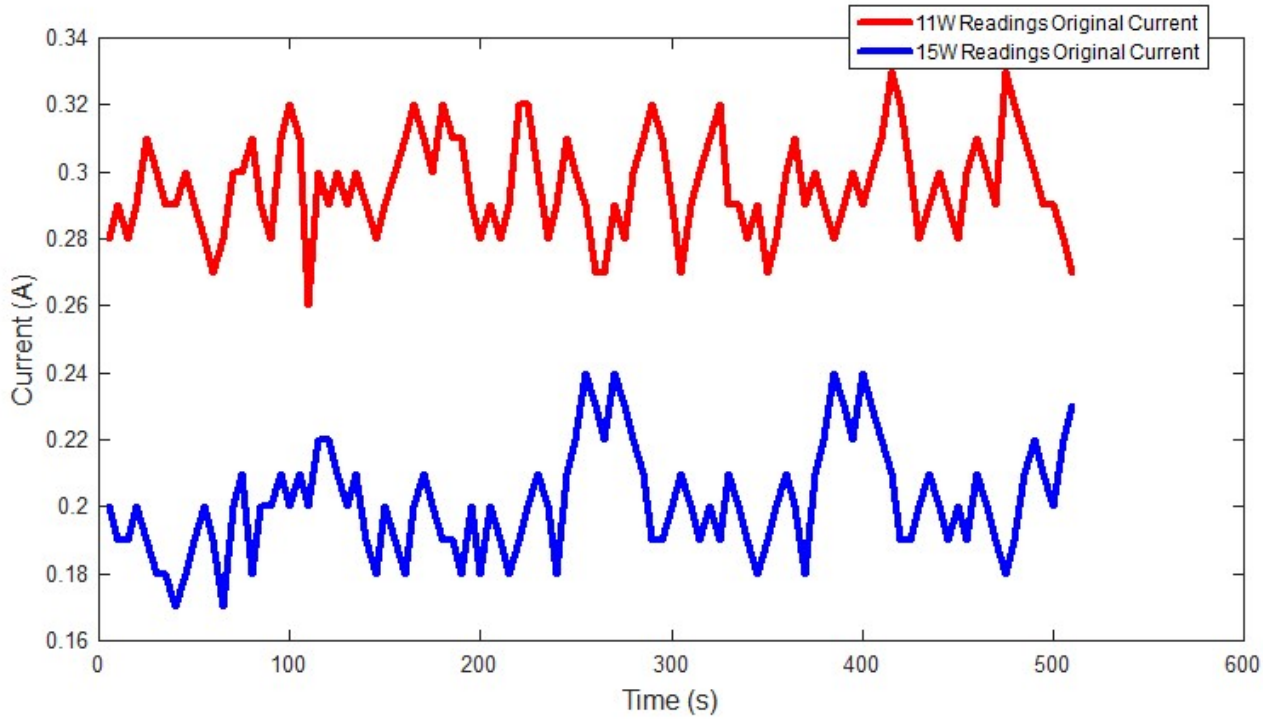

(b) 11W and 15W Current Waveforms

Figure 6: (a) 11W and 15W Voltage Waveforms; (b) 11W and 15W Current Waveforms.

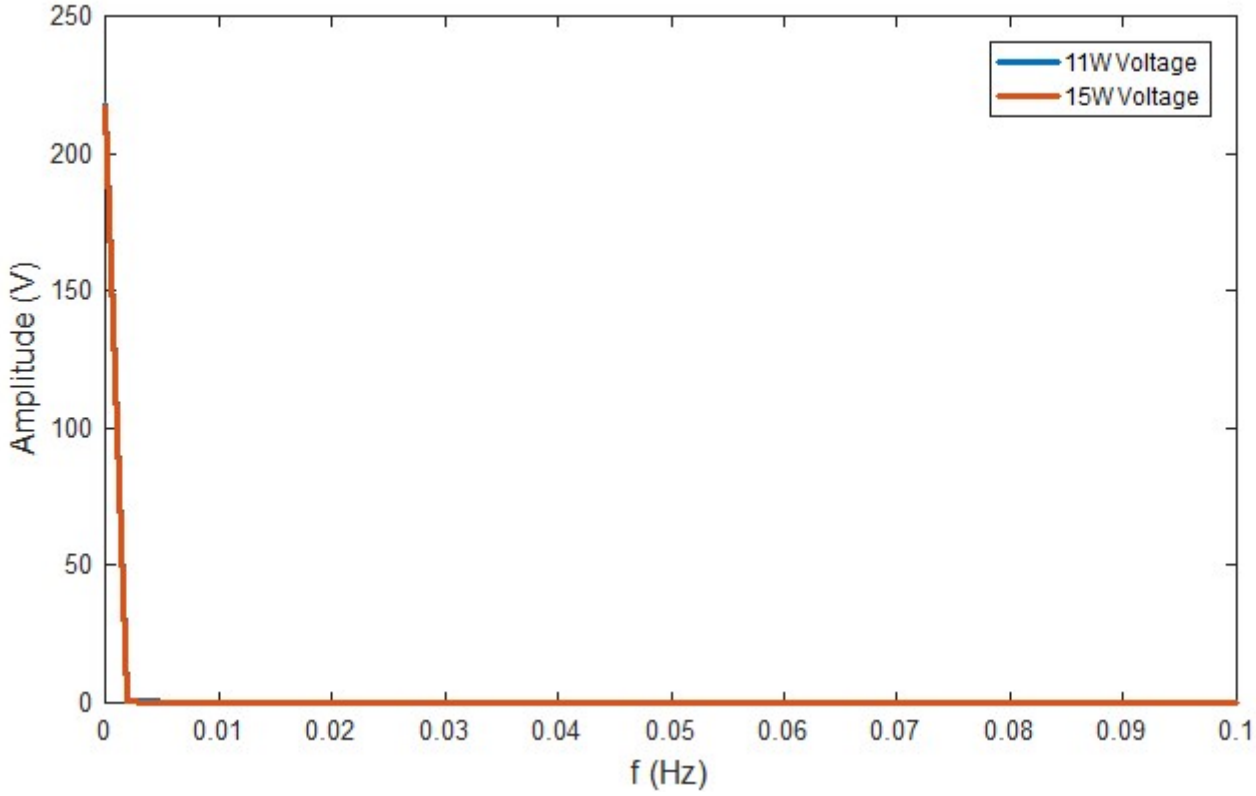

(a) Harmonic Voltage Spectrum of 11W and 15W CFL

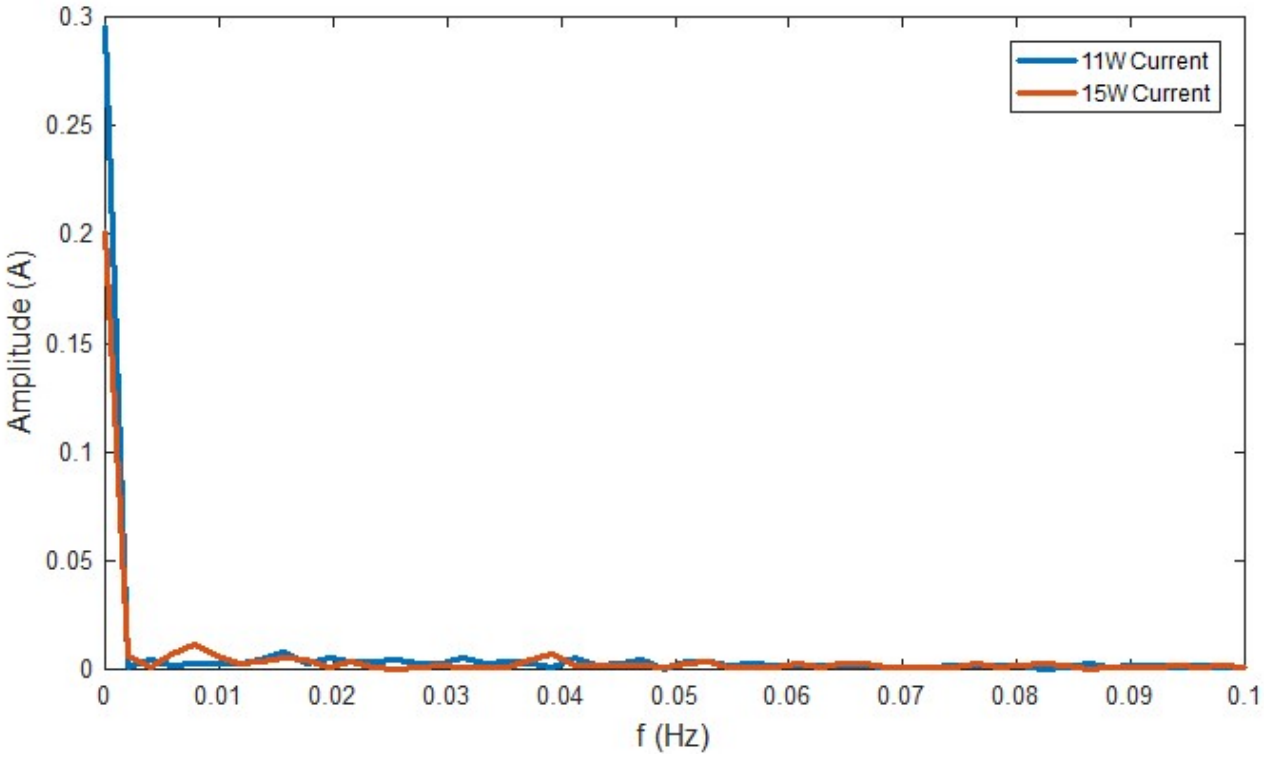

(b) Harmonic Current Spectrum of 11W and 15W CFL

Figure 7: (a) Harmonic Voltage Spectrum of 11W and 15W CFL; (b) Harmonic Current Spectrum of 11W and 15W CFL.

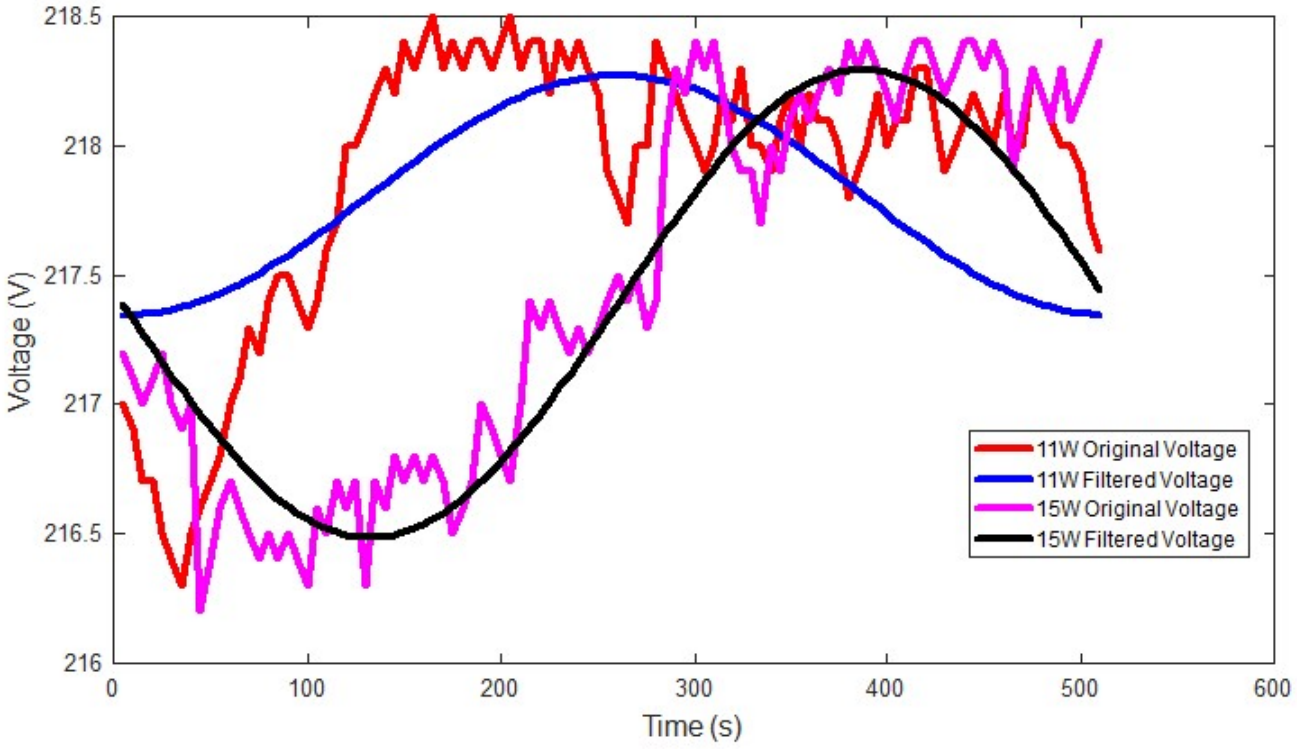

(a) Comparing the original voltage waveforms with the filtered waveforms

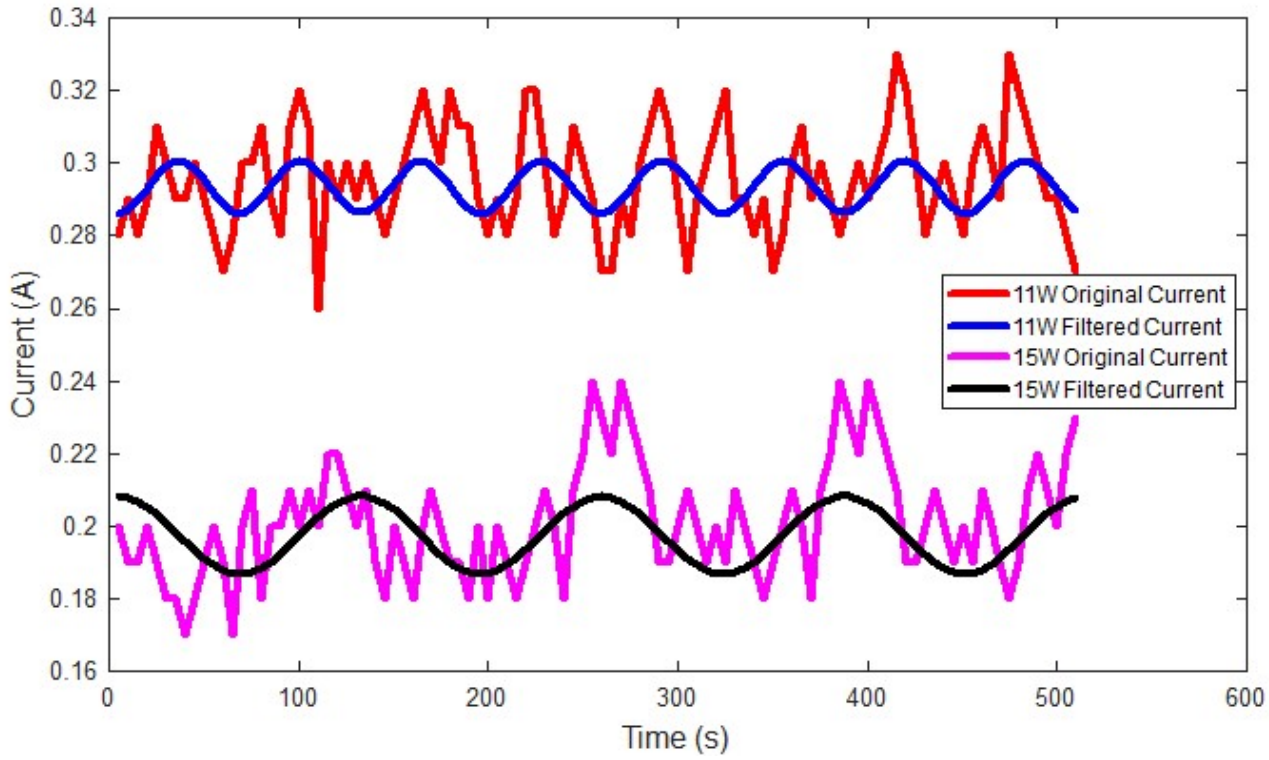

(b) Comparing the original current waveforms with the filtered waveforms

Figure 8: (a) Comparing the original voltage waveforms with the filtered waveforms; (b) Comparing the original current waveforms with the filtered waveforms.

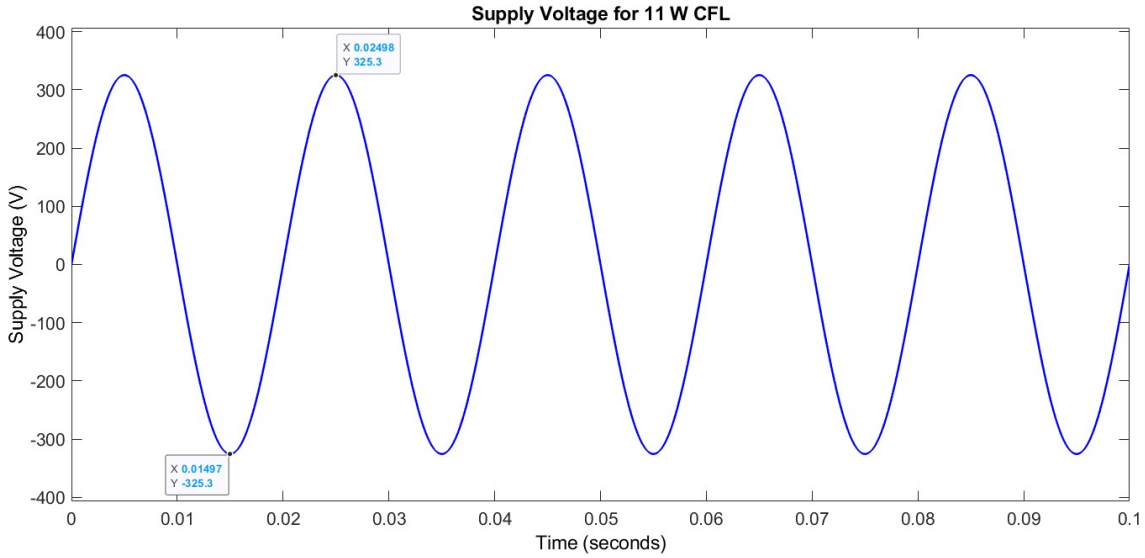

(a) Source voltage for the 11 W CFL

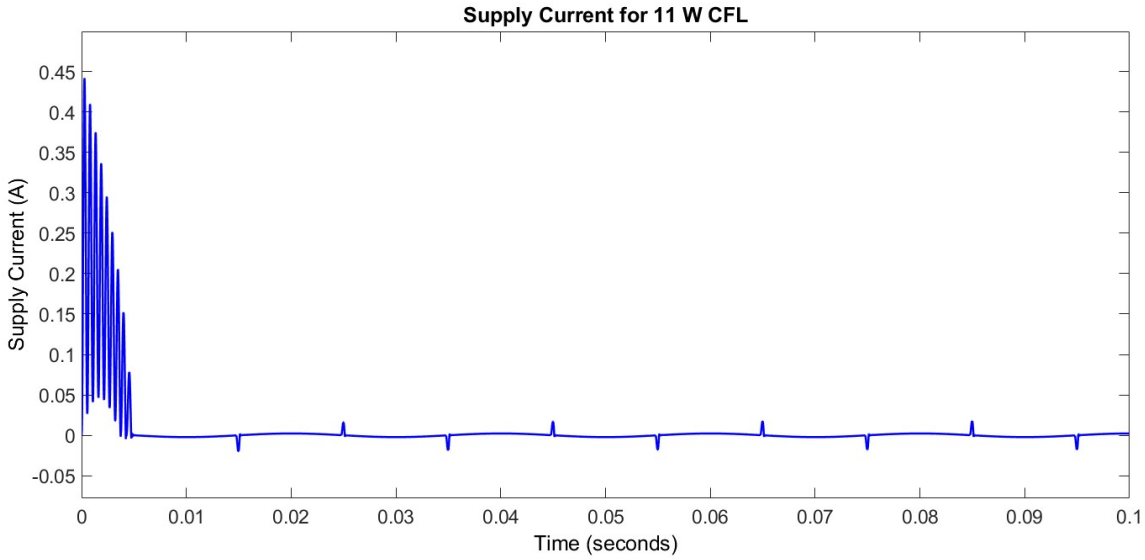

(b) Source current for the 11 W CFL

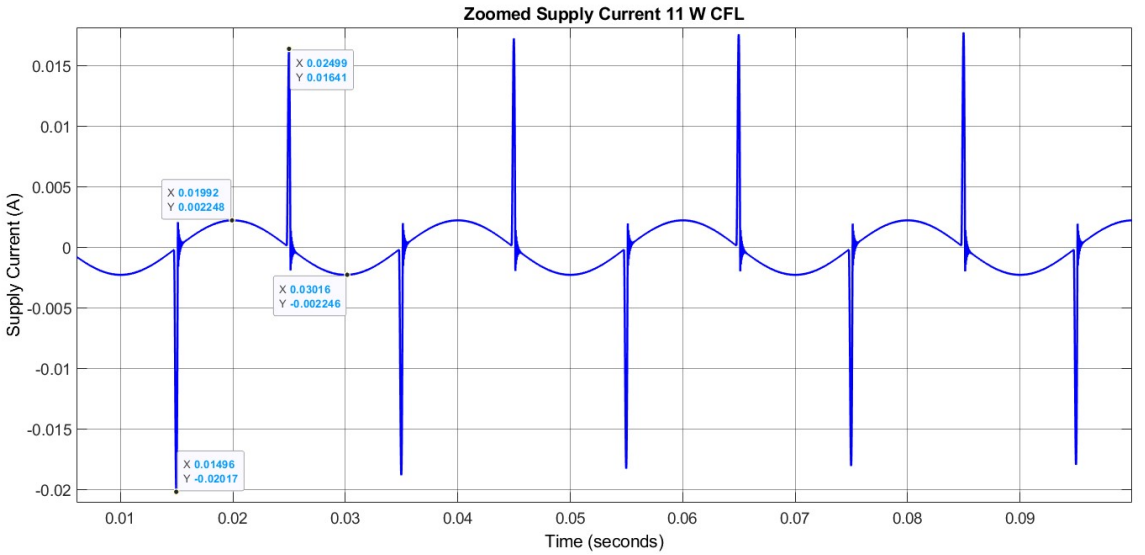

(c) Zoomed source current waveform for the 11 W CFL during running

Figure 9: (a) Source voltage for the 11 W CFL; (b) Source current for the 11 W CFL; (c) Zoomed source current waveform for the 11 W CFL during running.

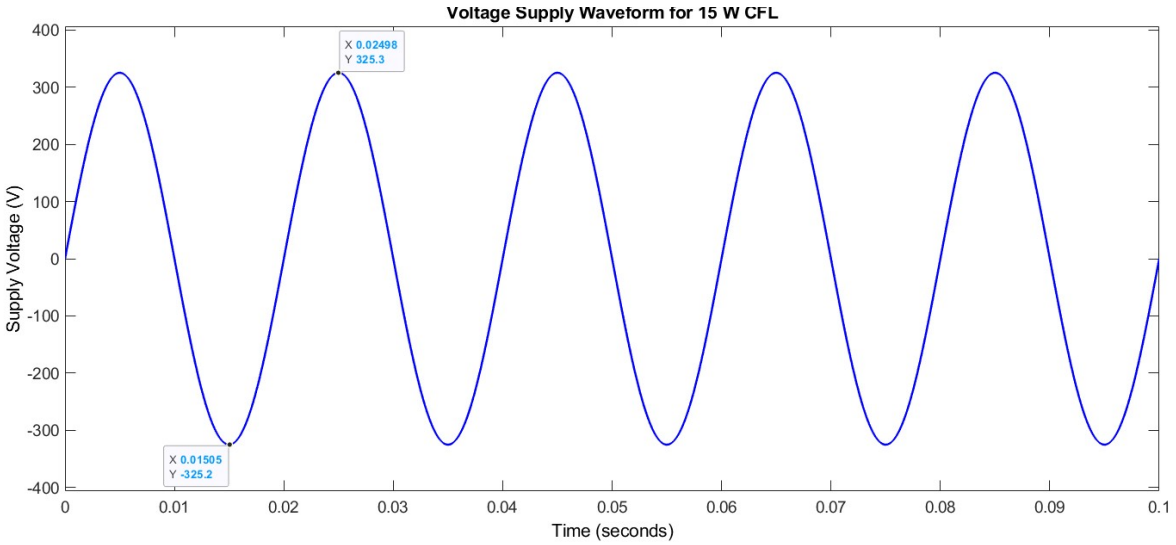

(a) Voltage supply waveform for the 15 W CFL

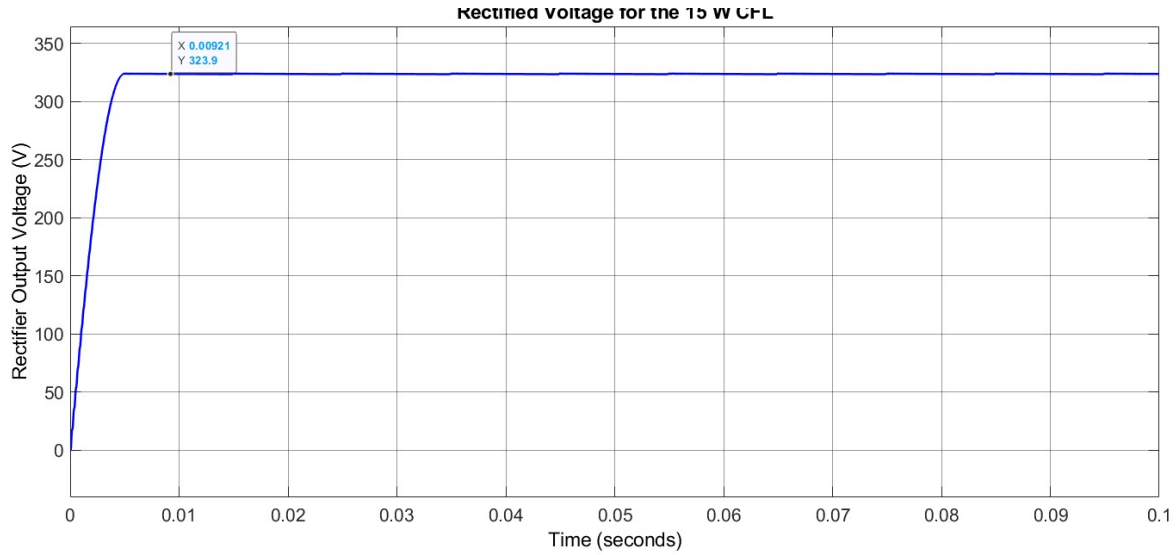

(b) Output voltage of the full-wave rectifier for the 15 W CFL

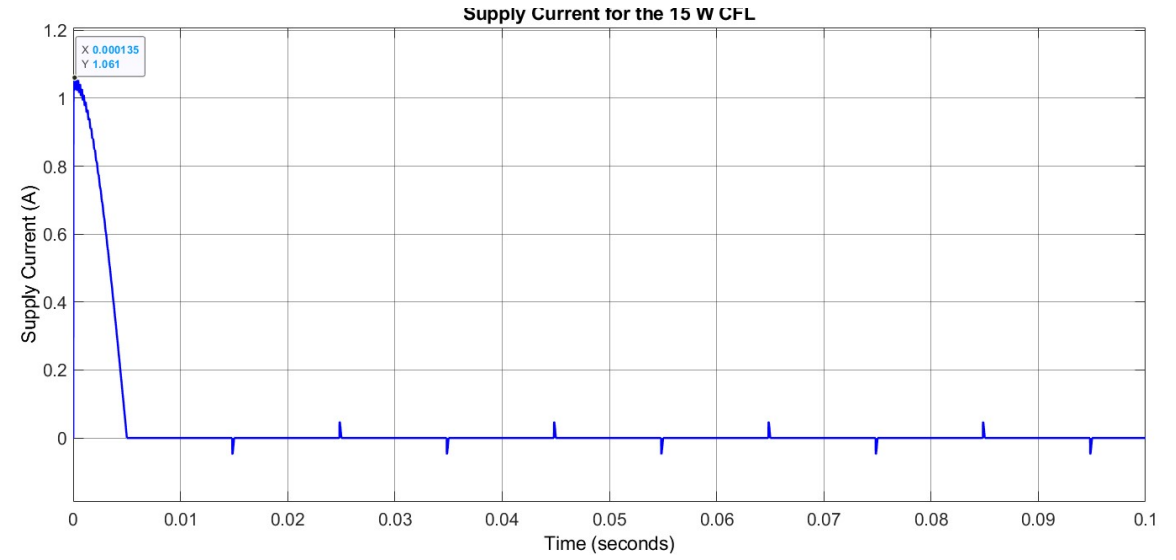

(c) Source current waveform for the 15 W CFL

Figure 10: (a) Voltage supply waveform for the 15 W CFL; (b) Output voltage of the full-wave rectifier for the 15 W CFL; (c) Source current waveform for the 15 W CFL

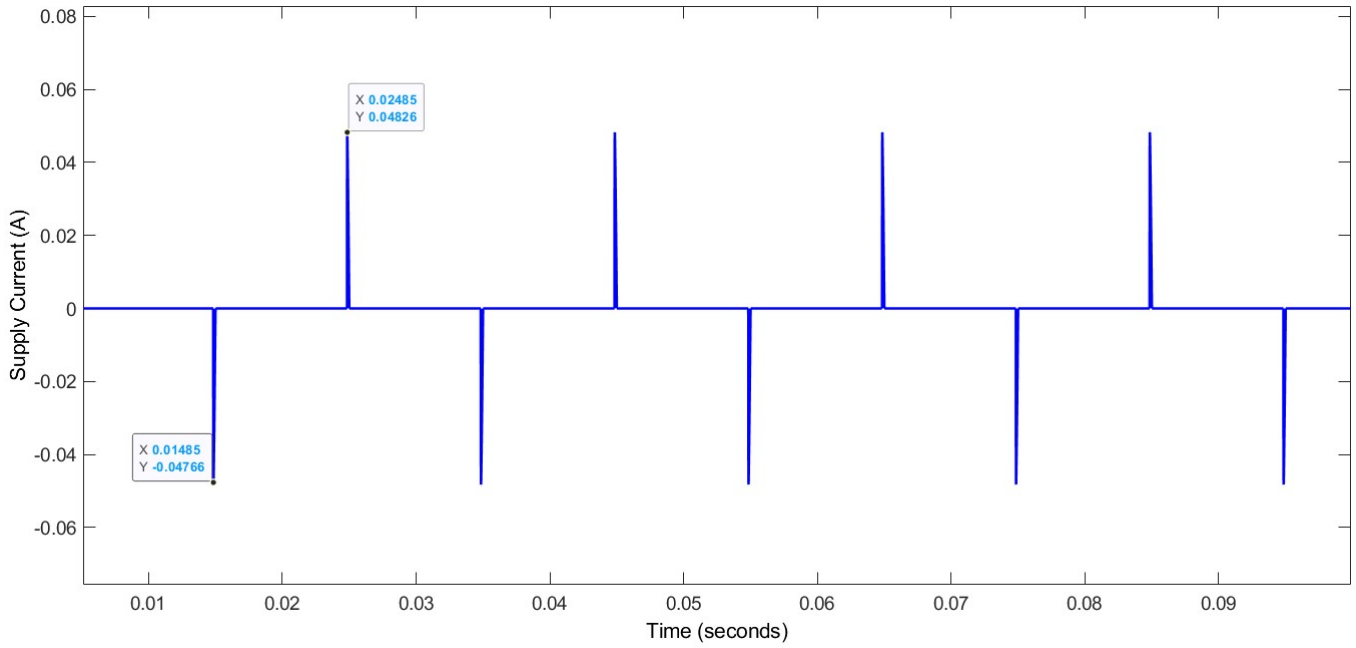

(d) Source current waveform for the 15 W CFL during running stage

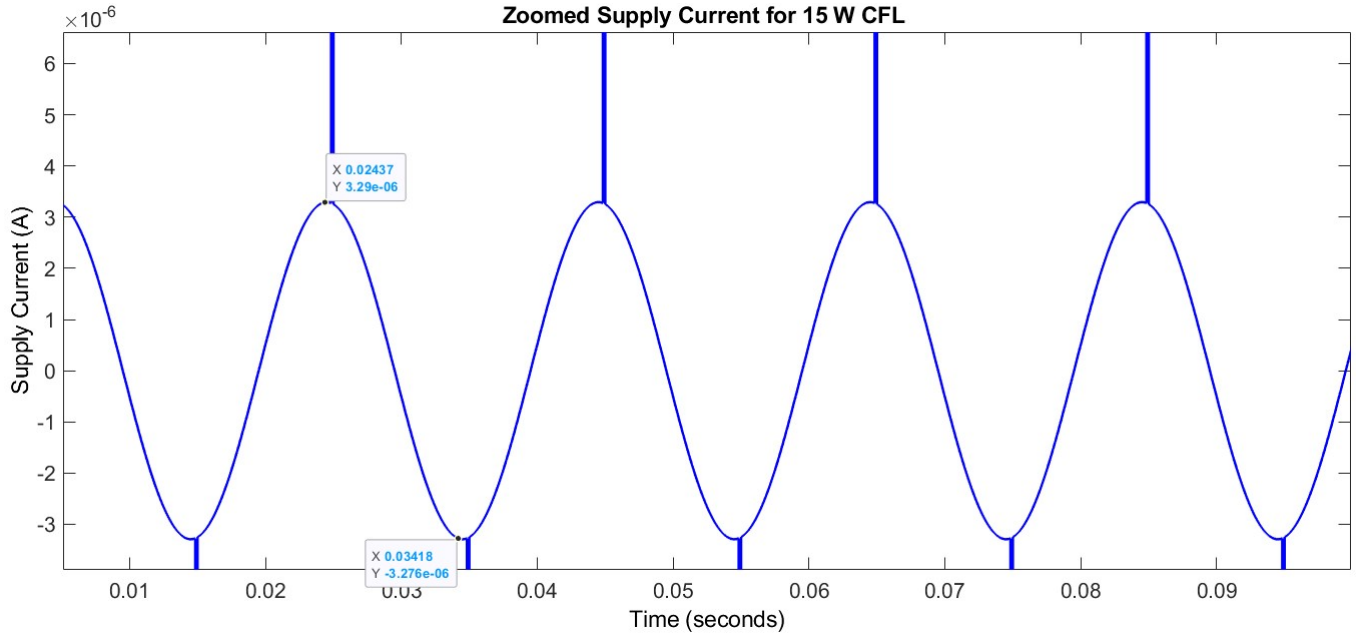

(e) Zoomed source current waveform of the 15 W CFL during running stage

Figure 10: (d) Source waveform for the 15 W CFL during running stage; (e) Zoomed source current waveform of the 15 W CFL during running stage.

maximum voltage amplitude is 218V. Fig. 7(b) displays the current waveforms in the spectral domain. The maximum amplitude of the 11W CFL is 0.3 A, while the maximum amplitude of the 15W is 0.2 A. The filtered signals in Figs. 8(a) and 8(b) were expressed in Eqs. (5) and (6) for the voltages and currents, respectively. Specifically, Eqs. (5) and (6) show that the voltage frequency (0.00196) of both CFLs are the same, whereas the current frequencies are different. This indicates that the wattage of a CFL does not affect the frequency of its voltage waveform. The frequency of the 11W CFL current (0.00157) is higher than that of the 15W CFL current (0.00784). This indicates that the higher the CFL wattage, the lower the frequency of its current waveform.

Figure 9(a) shows the source voltage response of the 11 W CFL. Similar to the 15 W CFL in Figure 10(a), there is little or no THDV in the source voltage. The THDV is 0.249 dB. This is 2.908% higher than the fundamental component or 102.908% of the fundamental component. Also, the peak voltage is 325.3 V. Similar to the 15 W CFL in Fig. 10(c), the starting current is significantly higher than the running current as shown in Fig. 9(b). As expected, the starting supply current of about 0.43 A is less than 1 A for the 15 W CFL. Also, the spike on the current waveform of about 20 mA is greater than the normal operating current of 2.2 mA as shown in Fig. 9(c). It can be observed that the operating current of 11 W CFL is greater than that of the 15 W CFL. This is due to different values of the mutual inductances of the transformer used and the resistances of the CFL coiled tube. The total harmonic distortion for the current (THDI) is 1.463 dB. This is 18.345% higher than the fundamental component or 118.345% of the fundamental component.

Figure 10(a) shows the source voltage waveform when the 15 W CFL load is connected. It can be seen that little to no imperfections are observed on the waveform. The total harmonic distortion for the voltage (THDV) for the 15 W CFL is 9.069×10^{-5} dB. This is 0.001% more than the fundamental component or 100.001% of the fundamental component. It can be seen that the maximum voltage is 325.3 V using Eq. (2). Figure 10(b) shows the DC voltage which is the output voltage of the full-wave bridge rectifier. The value is 323.9 V which is about 1.4 V less than the peak voltage as a result of the voltage drop across the diodes as explained in Eq. (4) and the EMI circuit which was implemented before the rectifier circuit. Additionally, the choke increases the input current into the CFL load during the starting stage of the CFL, as noted in Section 3.1.1 of this paper. As shown in Fig. 10(c), the supply current is greatly higher during starting (about 1 A) until around 5 ms when the current stabilizes. Figure 10(d) shows current spikes of up to 48 mA which is higher than the normal operating current of 3.3μA as shown in Figure 10(e). The total harmonic distortion for the current (THDI) is 5.951 dB. This is 98.404% higher than the fundamental component or 198.404% of the fundamental component. Additionally, results indicate that the major contributor to the THDI occurs during the start-up stage of the CFL. Finally, Table 2 compares the implemented 11 W CFL and 15 W CFL. It can be seen that the major difference between the two CFLs is the current total harmonic distortion (THDI). Therefore, it can be deduced that the THDI increases with an increasing rated power of the CFL or the aggregation of a number of the smaller rated CFLs.

5. CONCLUSION

In this study, analyses of the electronic circuits of 11W and 15W Futina compact fluorescent lamps (CFLs) have been presented. The existing literature works revealed that the analysis of the current and voltage waveforms in the spectral domain for the CFLs had not been given adequate treatment, and there is a need to fill this gap. Thus, the need to present a rigorous analysis of the electronic circuit of the ballast is not out of place. The goal is to analyze the current and voltage waveforms in the spectral domain and compare the results with experimental measurements. To achieve this goal, a GUI was developed in MATLAB for the CFLs circuits analyses. Experimental and simulation analyses of the electronic circuits of the CFLs model YPZ220/11-BMSP RR/RDD and YPZ220/15-BMSP RR/RDD were carried out to evaluate their electrical characteristics. Additionally, simulation analysis of the current and voltage waveforms in the spectral domain was presented and the results are compared with the experimental measurements. Generally, results show that the CFLs featured fairly distinct electrical characteristics. In particular, the 11W lamp consistently has a higher amplitude than the 15W lamp. However, both lamps show similar waveforms after 300 seconds. The maximum voltage amplitudes for both 11W and 15W CFLs are reasonably the same, reaching a peak value of 218V. Additionally, the current waveforms in the spectral domain gave a maximum amplitude of 0.3 A for the 11W CFL and 0.2 A for the 15W. Finally, the major difference between the two CFLs is the current total harmonic distortion (THDI). The THDI increases with increasing rated power of the CFL or the aggregation of a number of the smaller rated CFLs. Future work would focus on analyzing the harmonic characteristics and modeling of the Compact Fluorescent Lamps.

ACKNOWLEDGEMENT

Agbotiname L. Imoize is partly supported by the Nigerian Petroleum Technology Development Fund (PTDF) and the German Academic Exchange Service (DAAD) through the Nigerian-German Postgraduate Program under Grant 57473408.

References

[1] J. Lam, J. Hui, and P. Jain, "A dimmable high power factor single-switch electronic ballast for compact fluorescent lamps with incandescent phase-cut dimmers," *IEEE Trans. Ind. Electron.*, vol. 59, no. 4, pp. 1879–1888, 2012.

[2] J. Lam and P. Jain, "A simple single switch electronic ballast for compact fluorescent lamps with passive power factor correction (PFC) and soft switching capability," in *IECON Proc. (Industrial Electron. Conf.*, 2012, pp. 4503–4508.
[3] G. Ganandran, T. Mahlia, H. Ong, B. Rismanchi, and W. Chong, "Cost-benefit analysis and emission reduction of energy efficient lighting at the universiti tenaga nasional," *Sci. World J.*, pp. 1–11, 2014.
[4] J. Lam, S. Pan, and P. Jain, "A single-switch valley-fill power-factor-corrected electronic ballast for compact fluorescent lightings with improved lamp current crest factor," *IEEE Trans. Ind. Electron.*, vol. 61, no. 9, pp. 4654–4664, 2014.
[5] A. Vitanza, R. Scollo, and A. Hayes. (1999) Electronic fluorescent lamp ballast. [Online]. Available: http://www.st.com/content/ccc/resource/technical/document/application_note/43/99/f4/24/48/d7/41/7f/CD00003901.pdf/files/CD00003901.pdf/jcr:content/translations/en.CD00003901.pdf.
[6] B. Saršon, "Energy consumption of manufacturing line with special emphasis on lighting system," *Mälardlens Högskola*, pp. 1–83, January 2011.
[7] P. Bertoldi and C. Ciugudeanu. (2005) Successful examples of efficient lighting. Eur. Comm. DG JRC, Inst. Environ. Sustain. Renew. Energies Unit EUR. [Online]. Available: http://www.eu-greenlight.org/pdf/GL_Reports/GL_Report_2005.pdf.
[8] O. GmbH. (2014) Technical application guide - OSRAM. [Online]. Available: https://dammedia.osram.info/media/binx/osram-dam-505732/7129720.pdf%5Cnhttp://www.osram.com/osram_com/products/lamps/fluorescent-lamps/fluorescent-lamps-t8/lumilux-t8/index.jsp.
[9] E. Mills, "Energy-efficient lighting policies and programs from the united states government," in *Int. Light. Conf.*, 1995, pp. 1–12.
[10] P. Teodosescu, M. Bojan, I. Vese, and R. Marschalko, "LED Drive Technology Based on CFL Ballast Topology," *ACTA Electroteh.*, vol. 53, no. 3, pp. 235–241, 2013.
[11] F. Montoya and J. Castillo, "Power quality in modern lighting: Comparison of LED, microLED and CFL lamps," *Renew. Energy Power Qual. J.*, vol. 1, no. 14, pp. 500–505, 2016.
[12] E. Elijošiutė, J. Balciukevičiūtė, and G. Denafas, "Life cycle assessment of compact fluorescent and incandescent lamps: Comparative analysis," *Environ. Res. Eng. Manag.*, vol. 61, no. 3, pp. 65–72, 2012.
[13] R. Pfeifer, "Comparison between filament lamps and compact fluorescent lamps," *Int. J. Life Cycle Assess.*, vol. 1, no. 1, pp. 8–14, 1996.
[14] L. Nerone, "Novel self-oscillating class e ballast for compact fluorescent lamps," *IEEE Trans. Power Electron.*, vol. 16, no. 2, pp. 175–183, 2001.
[15] Z. Wei, N. Watson, and L. Frater, "Modelling of compact fluorescent lamps," in *ICHQP 2008 13th Int. Conf. Harmon. Qual. Power*, 2008, pp. 1–6.
[16] J. Yong, L. Chen, A. Nassif, and W. Xu, "A frequency-domain harmonic model for compact fluorescent lamps," *IEEE Trans. Power Deliv.*, vol. 25, no. 2, pp. 1182–1189, 2010.
[17] T. Oluwafemi, S. Gupta, S. Patel, and T. Kohno, "Experimental security analyses of non-networked compact fluorescent lamps: A case study of home automation security," Work. Learn. from Authoritative Secur. Exp. Results, LASER 2013, pp. 13–24, 2013.
[18] N. Rey-Raap and A. Gallardo, "Determination of mercury distribution inside spent compact fluorescent lamps by atomic absorption spectrometry," *Waste Manag.*, vol. 32, no. 5, pp. 944–948, 2012.
[19] D. Sarigiannis, S. Karakitsios, M. Antonakopoulou, and A. Gotti, "Exposure analysis of accidental release of mercury from compact fluorescent lamps (CFLs)," *Sci. Total Environ.*, vol. 435, pp. 306–315, 2012.
[20] R. Khan, R. Mccluskey, and R. Sung, "Evaluation of harmonic impacts from compact fluorescent lights on distribution systems," *IEEE Trans. Power Syst.*, vol. 1, no. 4, pp. 1772–1780, 1995.
[21] M. Dalla-Costa, R. Do-Prado, A. Seidel, and F. Bisogno, "Performance analysis of electronic ballasts for compact fluorescent lamp," in *Conf. Rec. - IAS Annu. Meet. (IEEE Ind. Appl. Soc.)*, vol. 1, no. c, 2001, pp. 238–243.
[22] P. Tam, S. Hui, and S. Chung, "An analysis and practical implementation of a dimmable compact fluorescent lamp ballast circuit without integrated circuit control," in *PESC Rec. - IEEE Annu. Power Electron. Spec. Conf.*, 2006, pp. 2–9.
[23] D. Parsons, M. Clarke, P. Glynn, D. Paustenbach, and L. Jones, "The environmental impact of compact fluorscent lamps and incadescent lamps for australian conditions," *J. Soc. Sustain. Eng. Inst. Engibeers*, vol. 7, no. 2, pp. 8–14, 2006.
[24] J. Cunill-Solà and M. Salichs, "Study and Characterization of Waveforms From Low-Watt («25 W) Compact Fluorescent Lamps With Electronic Ballasts," *IEEE Trans. Power Deliv.*, vol. 22, no. 4, pp. 2305–2311, 2007.
[25] J. Lam and P. Jain, "A high-power-factor single-stage single-switch electronic ballast for compact fluorescent lamps," *IEEE Trans. Power Electron.*, vol. 25, no. 8, pp. 2045–2058, 2010.
[26] D. Matvoz and M. Maksić, "Impact of compact fluorescent lamps on the electric power network," in *ICHQP 2008 13th Int. Conf. Harmon. Qual. Power*, 2008, pp. 4–9.
[27] L. Ramroth, "Comparison of life-cycle analyses of compact fluorescent and incandescent lamps based on rated life of compact fluorescent lamp," Rocky Mt. Inst., February 2008.
[28] D. Matvoz and M. Maksic, "Comparison of LED and CFL Lamps and Their Impact on Electric Power Network," pp. 320–327, 2012.
[29] T. Ribarich and J. Ribarich, "A new procedure for high-frequency electronic ballast design," *IEEE Trans. Ind. Appl.*, vol. 37, no. 1, pp. 262–267, 2001.
[30] P. Oramus, D. Smugała, and P. Zydroń, "Modeling of specific harmonics source in EMTP/ATP - case study of Compact Fluorescent Lamp," *Prz. Elektrotechniczny*, vol. 89, no. 8, pp. 320–324, 2013.
[31] J. Revelo-Fuelagán, J. Candelo-Becerra, and F. Hoyos, "Power factor correction of compact fluorescent and tubular LED lamps by boost converter with hysteretic control," *J. Daylighting*, vol. 7, no. 1, pp. 73–83, 2020.